Network Allocation of BESS with Voltage Support Capability for Improving the Stability of Power Systems

Nicolás Cifuentes [1], Claudia Rahmann [2,*], Felipe Valencia [2], Ricardo Alvarez[2]

[1] Control and Power Research Group, Electrical & Electronic Engineering Department, Imperial College London, London, United Kingdom
[2] Electrical Engineering Department, University of Chile, Av. Tupper 2007, Santiago, Chile
[*] crahmann@ing.uchile.cl

Abstract: **The stability of future power systems will be challenged by high shares of converter-based generation technologies (CBGTs). To prevent instability problems, it is essential to explore new technologies and control strategies able to counteract the negative effects that CBGTs may have. In this regard, promising technologies are battery energy storage systems (BESS), which can provide a wide range of benefits from a stability viewpoint. Current methodologies that quantify and allocate BESS in electrical networks have been developed from an economic perspective considering a steady-state formulation of the system. Accordingly, these allocation approaches do not exploit all the benefits that BESS can offer to system stability. This paper proposes a novel optimization methodology for efficient BESS allocation in systems with high levels of CBGTs. The model improves system stability by considering BESS with voltage support capability during contingencies. The allocation is solved by a genetic algorithm considering the transient voltages throughout the network busbars and their short circuit levels. The methodology was implemented in the 39 busbar New England system. Compared to traditional approaches, the proposed BESS allocation method enables significant improvements in the stability of the system during critical contingencies.**

Nomenclature

B_{ESS}	connection busbar of BESS
Z_{eq}^{sys}	power system equivalent Thévenin impedance
Z_f	fault impedance
V_0	power system voltage
V_f	fault voltage
V_{f0}	fault voltage without voltage support
I_{SC}^{sy}	power system current
I_{SC}	fault current
I_{BESS}	current injected by BESS
θ_{BESS}	phasor angle of I_{BESS}
θ_{sys}	phasor angle of Z_{eq}^{sys}
S_{BESS}	nominal power of BESS
S_{SC}^{sys}	short circuit level of the power system at bus B_{ESS}
i_{BESS}	per unit magnitude of the current injected by BESS
N_K	number of allocation busbars
N_C	number of critical contingencies
K_i	i-th busbar
λ_k	weighting factor of contingency k
U_{ik}^{g}	transient voltages at busbar i during contingency j with BESS allocation candidate g
U_{ik}^{0}	transient voltages at busbar i-th during the fault j without BESS
n_i	Number of BESS modules installed in busbar i
$\mathcal{B}$	Set of candidate busbars
$\mathcal{G}$	Set of busbars with synchronous generators
$\mathcal{K}$	Set of contingencies
j	Imaginary unit
N_{BESS}	number of BESS modules to be installed in the network
S_{mod}	installed capacity of each BESS module
N_Q	total number of allocation candidates in the search space
m	total number of genes to be mutated
N_g^{mut}	total number of modules to relocate in selected genes to be mutated
P_i^{mut}	probability of the i-th bus to be mutated
$\widehat{S}_i^{SC}$	reciprocal of the normalized shot circuit power of i-th bus (i.e. $\hat{S}_i^{SC} = 1/S_i^{SC}$)
N_p^g	total number of different offspring generated from the g-th parent
ΔN_p^g	total number of different offspring generated from the g-th parent

1. Introduction

For almost a century, power system stability has been recognized as one of the key issues for economic and secure power system operations. [1]. The uncontrolled, widespread, and cascading interruptions that may follow a contingency event involve huge economic and social consequences. For instance, the 2003 blackout in the U.S. resulted in the loss of 61.8 GW of electric load that was serving more than 50 million people and costed an estimated USD 6 billion [2]. Other major blackouts occurred in India (2012, 620 million people affected), Brazil (2011, 53 million people affected), and China (2008, 4 million people affected). Accordingly, energy regulators and system operators regularly perform different stability studies in order to detect hazardous situations and develop corrective measures. These corrective measures are designed to maintain system stability over a wide range of scenarios and thereby avoid the economic and social impacts resulting from major blackouts.

In power systems dominated by synchronous generators (SGs), the short circuit level at a given location is a common indicator of system strength: the higher its value, the higher the network strength at the pertinent node [3]. High fault current levels are found in strong power systems, while low levels are representative of weak networks [4]. The short circuit level is a metric that traditionally represents the

voltage stiffness of a network [5]. High short circuit levels indicate a strong system with stiff voltages, which means they will not deviate far from their initial values when subjected to small disturbances. This is because the series impedances of strong systems are relatively low and therefore the voltages are less sensitive to changes in power flows (dV/dP, dV/dQ) [6].

Even though short circuit levels are calculated using steady state values, they are a reliable measurement of how the grid's bus voltages are affected during contingencies [7]. Indeed, in power systems with high short circuit levels, there are a large number of SGs providing high fault currents and, thus, they support the stability of the grid. High short circuit currents flowing into the grid during a contingency event can be viewed as a "strong" response from the SGs to the voltage drops, which try to restore the system back to its normal operation [4]. The short circuit levels are then an accurate measurement of the strength of the system's response to different faults.

Historically, stability has been successfully sustained by SG contributions and by the control actions of the different controllers distributed throughout the network. However, this paradigm may not be sustained for long in modern power systems with high shares of converter-based generation technologies (CBGT). In these scenarios, stability problems may arise due to the fundamental differences between CBGT and conventional synchronous machines [6]. One key difference is the limited capacity of CBGTs to deliver fault currents. Their values range between 1.1 and 1.5 times their nominal current [8], which are significantly lower than the fault current that a SG can provide [9]. Given that in conventional power systems the synchronous machines are the major sources of short-circuit current contributions [5], their displacement by CBGTs will lead to an overall reduction of the system's strength [4]. The reduction of system strength leads to higher values of dV/dP and dV/dQ, meaning that small disturbances in the power flows can significantly change network voltages [6]. During contingencies, systems with low short circuit levels may experience extremely depressed voltages over a wide network area and then, after the fault clearance, they have difficulties recovering the voltages. Severe voltage dips may also considerably speed up the rotors of the nearby machines, which in turn may cause them to lose their synchronism. Accordingly, reducing system strength by increasing CBGTs can significantly impair the dynamic performance of the system during contingencies, thereby making the system more prone to stability problems [5]-[7], [10].

To prevent future instability problems in power systems with high shares of CBGTs, it is essential to explore new technologies and develop novel control strategies that can counteract the negative effects of CBGTs. This is the only way that their secure integration into modern energy systems can be ensured. In this regard, battery energy storage systems (BESS) are one of the most promising technologies that have received increasing attention lately [11]. Bulk BESS can provide the flexibility needed to deliver and accommodate renewable power efficiently [11], [12]. In addition, BESS are fast-responding devices that not only add more flexibility to frequency and voltage regulation, but also provide a wide range of technical benefits from a stability point of view [13]-[15].

Within the existing technical literature, considerable efforts have been made to assess the value that BESS can offer to power systems with high levels of CBGTs. Several of these works have focused on identifying the appropriate size and network location of BESS considering economic frameworks [11],[12],[16]-[22]. Although these studies represent an important step towards the efficient deployment of BESS in future power systems, the benefits that BESS can provide to system stability cannot be portrayed by economic approaches.

In the aforementioned context, this paper presents a novel optimization model for the efficient allocation of BESS in power systems with high levels of CBGTs. The model improves short-term voltage and rotor angle stability of the systems by increasing system strength. For this purpose, BESSs are modelled with *voltage support capability*, which means that they can support the stability of the system by injecting reactive current during short circuits. To overcome the modelling complexity of the optimization, we solved the allocation problem by a meta-heuristic algorithm based on a genetic algorithm (GA). The algorithm allocates the BESS modules to minimize voltage dips of the network during a set of critical scenarios, where short circuit levels are considered as a main allocation indicator. We implemented our model in the 39-bus New England system [23]. The results we obtained show that, compared to the traditional BESS allocation approaches, the proposed model enables significant improvements in the stability of the system.

The remainder of this paper is organized as follows: Section 2 presents a review of selected studies that identify and quantify the benefits of BESS in power systems. Section 3 presents the theoretical background needed to understand the contribution that BESS can provide in order to improve system stability. Section 4 presents the mathematical formulation of the optimization problem. Section 5 describes the proposed methodology for allocating the BESS. Section 6 summarizes the key aspects of the proposed optimization algorithm. Section 7 presents the case study. The results obtained are presented in Section 8 and finally the conclusions are drawn in Section 9.

2. Literature review

In this section, first we aim to identify the benefits that Energy Storage Systems (ESS) can bring to power system operations, seen from different perspectives. A second goal is to learn about the best ESS allocations when considering economic approaches.

2.1. Benefits of ESS considering economic frameworks

The evaluation of the benefits of BESS in power systems with high levels of CBGTs is an active research area that has received considerable amount of attention in recent years. Within expansion planning frameworks, the benefits of BESS have been researched in [11], [16]-[19]. The main conclusion found in these works is that ESS can reduce the investments needed for transmission and/or generation capacity, mainly because of their ability to provide greater flexibility to power system operation. The recommendations given by these works, in regards to the allocation of BESS, is to install them either in busbars with renewable generators or deploy them in busbars close to the load centers. Within operational frameworks, the benefits of BESS have been

studied in [12], [20]-[22]. These works have shown that BESS enable a higher utilization of the network infrastructure by providing flexibility to the demand supply management and offer support in case of contingencies. The economic viability of BESS is usually evaluated based on profits from arbitrage opportunities across the energy and ancillary markets. Regarding the allocation of BESS, these works usually locate them either on busbars with renewable generation, close to the load centers, or nearby congested corridors.

The body of literature that was reviewed indicates that the value and benefits of ESS strongly depend on market conditions, network configurations, and the degree of detail considered in the case studies. Consequently, the optimal BESS network allocation, i.e. the one that enables the extraction of the highest value from a systemic perspective, cannot be generalized. Still, two major trends were observed throughout the studies here reviewed: either to co-locate the BESS units together with wind and solar power plants or to place them in specific load buses. However, even if these trends in BESS allocations are the best from an economic perspective, nothing can be said about their performance in terms of system stability. Considering the economic and social impacts that major blackouts may have on society, it is worth investigating which are the best ESS locations if the objective is to improve the stability of the system.

2.2. Benefits of ESS for improving system stability

Traditional mechanisms to improve power system stability can be categorized in [24], [25]:

- Control strategies implemented in SGs such as Power System Stabilizers (PSS) and fast valving actions.
- Flexible AC Transmission (FACT) devices that increase the stability margin of the system.
- Special Protection Schemes (SPS), with improved coordination and more redundancy in the network.

Control strategies applied to SGs such as PSS provide additional damping to the rotor swings during large disturbances, improving the system's transient stability [24]. FACT devices on the other hand, can be used as a preventive measure to system instability. FACTS can increase the steady state stability margin of the system, which is achieved by providing voltage controllability and also by enhancing the system's power transfer capability. Their fast switching characteristic also allows them to provide damping to power oscillations during large disturbances [24]. Finally, as a preventive measure for stability, TSO's might also implement SPS once stability assessment studies have been performed and the potential unstable operating conditions are identified [25].

In response to the new stability challenges introduced by large amounts of CBGTs, recent studies have started to assess the use of BESS in order to improve system stability as an additional alternative to the traditional approaches. To this end, most works have focused on developing new control strategies for BESS [13], [14], [26], [27]. In [13], a passivity-based non-linear control strategy was presented for a multi-machine power system in order to improve transient stability and provide voltage regulation. The control scheme was evaluated in a simple two-area system with 11 buses, 2 synchronous generators, 2 wind turbines, and one BESS unit located between both areas. This study's results show that the integration of BESS using their proposed control design method provides additional damping to the system, compared to other state-of-the-art linear and non-linear controllers. In [14], a multi-objective Lyapunov-based nonlinear controller for a STATCOM integrated with a BESS was presented. The controller was tested in a modified IEEE 14-bus system with one BESS unit located at a given bus. Their results show that the BESS helps to improve the generator rotor speed and voltage responses, which are significantly more damped, thus, improving the system transient stabilization. In [26] the authors propose a control scheme for BESS using wide-area information to improve the transient stability of the system. The controller uses the energy function and the rotor speed of the critical machine as stability indicators. The control scheme was tested in a modified IEEE RTS-24 system. To evaluate the benefits of the BESS controller, two case studies were conducted: in the first one, two BESS (with 100 MVA capacity) were installed in two given buses and in the second one, ten BESS modules (each one with 20 MVA capacity) were distributed in the network. Their results show that in both cases the system transient stability improved, compared to a traditional control system, but a distributed installation (with same total capacity) is preferable from a stability perspective. A similar control scheme for BESS was proposed in [27] for improving angle and voltage stability. In this case, the controller monitored the internal voltage and the rotor speed of the generators. Numerical examples were carried out using a multi-machine 10-bus test system, considering seven BESS modules distributed at load buses. Several case studies were simulated, each one with different BESS capacities. Their results show that, when using the proposed control scheme, BESS can improve both rotor angle and short-term voltage stability.

As concluded from the literature review, most works seeking to improve system stability by BESS propose new control strategies. These new BESS control schemes are designed and tested in small systems and consider a fixed distribution of BESS in the grid. So far, no previous research has proposed an optimization model that allocates BESS for the purpose of improving system stability, impeding us to fully explore the capabilities of BESS to increase system stability.

3. Stability support provided by BESS

This section aims to explain how the stability of power systems can be improved by means of BESS and what factors affect the degree of improvement. For this purpose, it is assumed that BESS supports system stability by injecting reactive current during short circuits. Since these devices can change very fast from a P –control mode to an I^q–priority control mode, BESS could maintain the stability during faults even if they are normally used for regulating the voltage or frequency. Moreover, in the future, this stability support capacity is expected to be remunerated as an ancillary service, and therefore, it will become an attractive option for BESS investors.

3.1. Effects of BESS as a function of the short circuit level

To assess the level of stability enhancement that a single BESS device can achieve, the circuit in Fig. 1 shows where the power system is represented by its Thevenin

equivalent. Without loss of generality, a three-phase short circuit is assumed at node B_{BESS}.

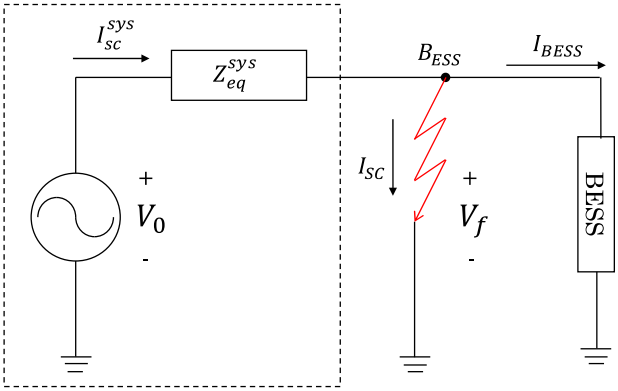

Fig. 1. *Circuit used to assess the contribution of BESS during faults.*

The voltage increase caused by the voltage support from the BESS can be written as a function of the short-circuit power of the system and the nominal power of the BESS, as follows [28]:

$$\eta = 1 - i_{BESS}\frac{S_{BESS}}{S_{sc}^{sys}}e^{j(\theta_{BESS}+\theta_{sys})} \qquad (1)$$

As seen in (1) the best case scenario, from a voltage support perspective, is $i_{BESS} = 1.0\ p.u.$ and $\theta_{BESS} + \theta_{sys} = \pi$. If we now consider the strongly inductive component of high voltage networks, the best angle for current injection is $\theta_{BESS} = \pi - \theta_{sys} = \pi/2$, which, in turn, means only reactive current injection from the BESS during the fault. Fig. 2 represents a voltage dip at node S_{BESS} with and without voltage support for different values of B_{BESS} and S_{SC}^{sys}. The results are computed assuming the best case, from a voltage support perspective, i.e., $i_{BESS} = 1.0$ and $\vartheta_{BESS} = \pi/2$. As seen in Fig. 2, a) faults occuring near the BESS connection point, i.e. where the residual voltage is low, the improvement achieved in the voltage dip caused by the BESS support is minor. This conclusion is independent from the ratio between the BESS installed capacity, S_{BESS} and the short circuit level of the system at the connection point, S_{SC}^{sys}. This implies that for faults close to the BESS, their support becomes inefficient.

Fig. 2 b) also shows that in the case of faults occurring far from the connection point of the BESS, voltage dips during the fault can be considerably improved with BESS support. Moreover, for a given BESS capacity, this improvement increases as the short circuit level of the system at the connection point S_{SC}^{Sys} decreases, i.e., as the system becomes weaker. This suggests that the BESS capacity should be allocated in weak areas of the system where voltage support will be more effective.

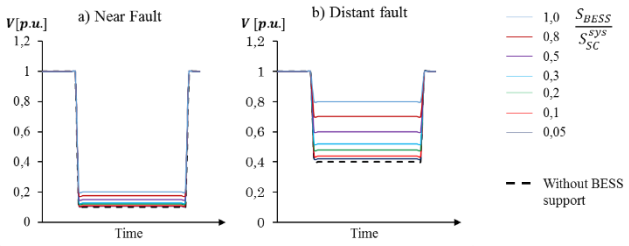

Fig. 2. *BESS contribution to the improvement of the voltage dip at its connection point.* ***a)*** *Fault nearby to the BESS,* ***b)*** *Fault far away from the BESS.*

3.2. Main conclusions

From the previous analysis the main outcomes are: 1) For faults that occur electrically close to the connection point of the BESS, their stability support becomes inefficient. Accordingly, the optimization process must consider several contingencies. Otherwise, relevant busbars from a stability perspective may be discarded during the BESS allocation. 2) In the case of faults that occur far from the BESS location, the voltage dip during the fault can be considerably improved through the BESS support, especially in weak areas of the system. Hence, it is expected that more BESS modules are located in busbars of the network with low short circuit levels. The short-circuit levels of the system can thus be used in the optimization process to guide the search and make it more efficient.

The previous analysis gives good insights on how the allocation problem should be addressed in order to maximize the benefits of BESS on system stability. However, to obtain the voltage dips on the entire network during several short circuits, we do not use (1). Instead, we use a short-circuit calculation methodology as explained later in section 4.

4. Mathematical formulation of the problem

4.1. Introduction

As mentioned in section 1, this work proposes a novel optimization model for efficient allocation of BESS in power systems with high levels of CBGTs. The model improves the stability of the system by increasing system strength for a set of critical scenarios. For this purpose, BESS are modelled with *voltage support capability*, which means that they support the stability of the system by injecting reactive current during short circuits.

The stability support provided by the BESS modules during faults can reduce voltage dips during contingency events. The reduction of the voltage dip in a specific busbar can be understood as a localized enhancement of the network strength at the pertinent node. Consequently, if several BESS modules are properly allocated in the network, the voltage dip throughout the entire system can be reduced. An increase in the network's strength translates into lower voltage dips during short circuits which. in turn, leads to a better voltage recovery after the fault clearance. Moreover, the improvement of voltage dips allows a higher power transfer to the system from the nearby generators, thus increasing their synchronizing torque. Thereby, the rotor angle stability of these generators can also be enhanced.

4.2. Optimization

In general terms, our proposed optimization algorithm allocates the BESS modules in such a way that they increase voltages during a set of short circuits, in comparison to not having BESS in a base scenario. The voltage increase is obtained due to the voltage support capability of the BESS allocated throughout the grid. Thus, the optimization maximizes the increase of the voltage that can be achieved in contrast to the base scenario.

To overcome the computational complexity involved in time-domain simulations, we estimated the voltage during the faults using the short-circuit calculation method presented in [30]. Accordingly, the optimization problem is as follows:

$$\max_{\{n_i\}_{i\in\mathcal{B}}} \sum_{j=1}^{N_C} \lambda_k \left[\sum_{i=1}^{N_K} \left(|U_{ik}| - \left|U_{ik}^0\right| \right) \right] \tag{2}$$

s.t.

$$\boldsymbol{Z_k}(\{n_i\}_{i\in\mathcal{B}}) \cdot \boldsymbol{I_k} = \boldsymbol{U_k}, \forall k \in \mathcal{K} \tag{3}$$

$$I_{ik} = n_i \cdot \frac{S_{mod}}{S_{base}} \cdot 2 \cdot (1 - |U_{ik}|) \cdot j, \forall k \in \mathcal{K}, \forall i \in \mathcal{B} \tag{4}$$

$$\sum_{i=1}^{N_K} n_i = N_{BESS} \tag{5}$$

The objective function (2) aims at maximizing the average voltage for all the contingencies on the basis of allocation decision variables $\{n_i\}_{i\in\mathcal{B}}$. In (3), $\boldsymbol{Z_k}$ represents the impedance matrix during contingency k, which depends on the fault type, its location and its impedance. The impedance matrix $\boldsymbol{Z_k}$ also depends on the allocation decision $\{n_i\}_{i\in\mathcal{B}}$, given the impedance of the transformers used to connect the BESS modules in the respective busbars. The column vectors $\boldsymbol{I_k}$ and $\boldsymbol{U_k}$ contain complex currents I_{ik} and complex transient voltages U_{ik}, respectively. Following the short-circuit calculation assumptions [30], the load currents are neglected and the system's synchronous machines are modelled as ideal voltage sources behind their transient reactances, i.e. $U_{ik} = 1\ [pu]\ \forall i \in \mathcal{G}$. On the other hand, the BESS modules are modelled as current sources with pure reactive current injection according to (4). Equation (4) represents the FRT requirements of the German Grid Code for voltage support [31]. Note that our formulation is not restricted to the German Grid Code, other voltage support schemes could be considered as well. Finally, constraint (5) forces the deployment of all available BESS modules.

The allocation problem (2)-(5) is a mixed-integer, non-linear, non-convex and large-scale optimization problem. In particular, the size of the problem is defined by: 1) how many BESS modules must be allocated N_{BESS}, 2) the set of allocation candidate busbars $\mathcal{B}$, 3) the set of contingencies $\mathcal{K}$ and 4) the amount of operating conditions considered in the optimization. Therefore, its solution poses significant computational challenges, especially in case of using reasonable-sized power systems. To overcome this complexity, we developed a solution methodology based on a genetic algorithm (GA).

5. Proposed methodology

Fig. 3 shows a block diagram of the proposed methodology. The input data contains the network topology, the power system components, the yearly operating conditions, and the total BESS capacity S_{BESS} that shall be distributed. The following subsections describe the main steps of the proposed methodology.

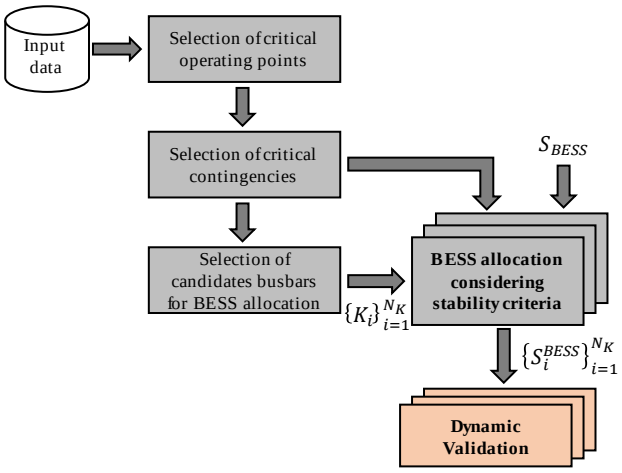

Fig. 3. *Methodology for network allocation of BESS*

5.1. Selection of critical operating conditions

To keep the problem computationally manageable, the first step of our methodology is to reduce its size. In order to do so, we first identify and select the critical operating conditions of the system to consider them within the optimization process. These operating conditions must be able to represent credible critical conditions that the power system may experience, from a stability perspective. Considering high levels of CBGTs, stability problems are most likely to occur during periods of low load and high levels of CBGTs, in which case a limited number of SGs would be operating to support the system's stability [32]. Thus, operating points characterized by low levels of net load should be selected. Also, situations with high load levels that may lead to heavily loaded transmission lines. Therefore, these cases are also considered in the solution of the optimization problem.

5.2. Selection of critical contingencies

Once the operating conditions are determined, the second step is to select a set of critical contingencies that will be included in the optimization process. The kind of contingencies under consideration are the typical faults used in stability assessments including three-phase short circuits in heavily loaded transmission lines that are near the highly loaded SGs. Once all the possible contingencies are taken into account, the selection is finally performed considering the critical network busbars and generators.

Critical busbars are identified by calculating their steady-state voltage stability margin over all the operating conditions under study. Then, those busbars that systematically present low margins are initially selected. The critical clearing times (CCT) are then calculated for 3-phase short circuits by means of time-domain simulations. However, they can also be estimated by means of other methodologies such as Lyappunov-based energy methods or using machine learning algorithms [33]-[35]. Then, the short circuits with the shortest CCT are selected.

The set of critical contingencies also includes 3-phase short circuits at the connection point of critical SGs. Critical

generators are those that lose synchronism when a short circuit occurs at their connection point. The identification of the critical SGs is performed based on their CCT, which is also calculated by means of time-domain simulations.

5.3. Selection of candidates busbars for BESS allocation

Once the critical operating conditions and contingencies have been selected, a further reduction of the problem size is performed by narrowing down the number of candidate busbars K_i to allocate the BESS. According to the theory presented in section 3, the approach should be to select the weakest busbars of the network because that is where a more efficient voltage support from the BESS is expected. In this context, the busbar's short-circuit level is a criterion to select weak busbars candidates and allocate the BESS. In [6], weak-area screening indicators are proposed on the basis of the short-circuit ratio (SCR) between the capacity of CBGTs to be installed and the short-circuit level at the connection point. Busbars with low SCRs are considered to be weak and thus CBGTs connected there have a higher risk of facing unstable operations [6]. In a similar manner, the authors of [29] show that busbars with low short-circuit levels are prone to experience both transient and voltage stability problems. Considering references [6] and [29], as well as the analysis presented in section 3, the weakest busbars of the network are selected as candidates for the allocation of the BESS, based on their short-circuit levels. Finally, the network's stronger busbars, near critical SGs that may become unstable, are also considered as candidates. These busbars are included in the optimization in order to avoid overlooking rotor angle instability of critical SGs.

5.4. Last steps

Once the problem size has been reduced, the BESS allocation for improving system stability can be performed. The proposed optimization algorithm is presented in detail in the next section.

As shown in Fig. 3, the last step of the proposed methodology is to validate the obtained BESS allocation through time-domain dynamic simulations.

6. Proposed algorithm for BESS allocation

The complexity of the mathematical formulation presented in (2) – (5), makes it extremely challenging to solve using traditional mathematical optimization methods, or without performing major simplifications that may affect the quality of the results. This justifies the use of an heuristic approach. In this context, GAs appear as a sound alternative for its solution, since integer variables can be easily codified as chromosomes. Moreover, GAs also allow us to evaluate the allocation candidates straightforwardly using different softwares such as PowerFactory DIgSILENT and, therefore, account for the non-linearities of the problem. More specifically, DIgSILENT allows us to perform short-circuit calculations using the methodology described in the UK Engineering Recommendation ER G7/4 [9]. This methodology is more sophisticated than the one described in [30], and allows us to include the reactive current support of BESS modules in order to obtain the transient voltages of the system during a short circuit. It is worth noticing that the methodology is not restricted to GAs or DIgSILENT. Other meta-heuristic algorithms and softwares can be used as well.

In order to solve the BESS allocation problem, a suitable GA was designed. The block diagram of the proposed GA is shown in Fig. 4. Although GAs cannot ensure optimality, they do provide a widely accepted and practical way of finding good solutions when solving complex optimization problems. However, their successful application for solving each particular problem requires extensive knowledge and experience, as well as a comprehensive analysis of the problem in question. Only by incorporating task-specific knowledge, GAs can be successfully used and applied to solve complex problems. The next sections include details about the formulation of the optimization and key issues regarding the design of the GA.

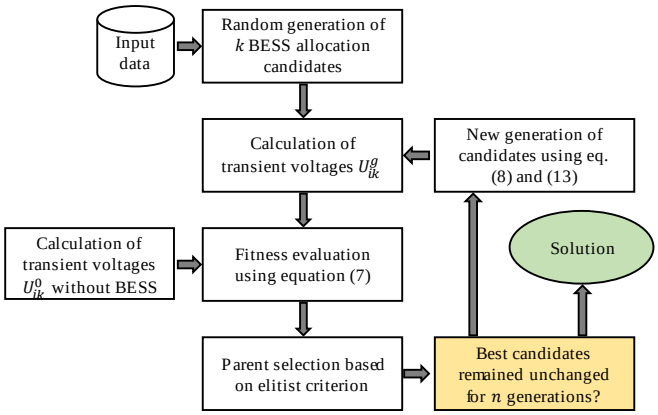

Fig. 4. *Block diagram of the proposed genetic algorithm.*

6.1. Fitness Function of the Genetic Algorithm (GA)

As already mentioned, the main objective of the optimization process is to allocate the BESS modules in order to decrease voltage dips within the network during a set of contingencies defined a priori (steps 1 and 2 of the methodology presented in Section 5). This allows enhancing the voltage recovery immediately after a fault clearance and it also reduces the acceleration process experienced by the SGs during the fault. Accordingly, short-term voltage and transient stability can be enhanced.

The GA models the allocation candidates as an array of integer numbers (chromosomes). Each gene of the chromosome corresponds to one busbar of the network where an integer number of the BESS modules can be located. According to this modelling approach, the total amount of allocation candidates in the search space is defined by the following equation:

$$N_Q = \binom{N_{BESS} + N_K - 1}{N_K - 1} \tag{6}$$

Equation (6) characterizes the combinatorial explosion of the search space as more modules or busbars are considered in the optimization.

The purpose of the fitness function is to decrease the voltage dip during a set of critical contingencies by connecting BESS to some busbars in the network. To do this, the fitness function considers the difference between the transient voltage with and without BESS, as follows:

$$fitness(q_g) = \sum_{j=1}^{N_C} \lambda_k \left[\sum_{i=1}^{N_K} (|U_{ik}| - |U_{ik}^0|) \right] \tag{7}$$

The transient voltages during a short circuit are calculated using the complete method as described in [9].

6.2. Operators of the Genetic Algorithm (GA)

6.2.1. Crossover operator: The crossover operator generates a new offspring (new candidate for the BESS allocation) from more than one parent solution. This is done by exchanging sections of genes between two "parent" candidates in order to generate a new "offspring" candidate. The best way to perform the crossover exchange is still an open discussion topic. In general, the simplest way is to define a static crossover cut and then to create new candidates by randomly selecting parents according to their fitness and recombining their genes. However, in this case the optimization requires satisfying the equality constraint by using the exact BESS modules available for the allocation problem (5). Consequently, it is not possible to systematically define –in an easy way– the crossover cut between two candidates to generate a new feasible offspring [36]. One way to avoid this issue is to generate a random crossover and then include a penalty in the fitness function for non-feasible candidates. However, this can lead to a premature convergence of the algorithm [37]. Therefore, this work does not consider the crossover operator. Here, only a single candidate is selected as parent for the next generation. To select the parent of the next generation, an elitist criterion is chosen [37]. This in turn means that once a new generation is created, its current parent will be replaced if and only if the best new offspring has a better fitness than his father. Otherwise, the parent remains unaltered. New generations are created by mutating the current parent via the mutation operator. For doing this, we incorporate the short-circuit levels of the power system in the design of the mutation operator in order to obtain a sound trade-off between exploitation and exploration [38]. Further details regarding this method are presented in the next section.

6.2.2. Mutation operator: The mutation operator is used to maintain the genetic diversity from one generation to the next. Mutation alters one or more genes in a chromosome in order to create new candidates. To do this, a number of m genes from the parent must be selected randomly to relocate the total number of modules available in those genes. The genes that will be mutated should be chosen to increase the exploration through the evolution process. To do this, in our proposed GA model, those buses with larger amounts of BESS modules mutate more often. As explained in Section 3.2, the support provided by BESSs is more effective when the busbars where they are connected become weaker (i.e. low short circuit level). The system's areas with low short-circuit levels are the most prone to face voltage and transient stability problems. This fact unveils the risk of premature convergence to local or non-desirable solutions, where the BESS modules are concentrated in a small set of weak buses of the network.

To avoid premature convergence of the algorithm to local optima and improve its ability to find good solutions, the probability that each bus gets mutated during the optimization process, is inversely proportional to its short-circuit power. This probability represents the chance of a busbar of being randomly chosen to redistribute its BESS modules to the rest of the busbars. According to this strategy, the mutation operator of the GA will mutate the weakest nodes of the network (i.e. those with the lowest short-circuit levels) more often. Therefore, we define the probability of the i-th bus to be randomly chosen to mutate as the reciprocal of its normalized short-circuit power, as follows:

$$P_i^m = \frac{\hat{S}_i^{SC}}{\sum_{i=1}^{N_K} \hat{S}_i^{SC}} \tag{8}$$

This design enables one to achieve a sound trade-off between exploitation and exploration throughout the evolution process without the need to adjust the parameters as usual in the case of GAs [39].

6.2.3. Exploration-exploitation trade-off: As mentioned in Section 6.2.1, since crossover operations are not considered in the GA, it is necessary to find a way to achieve a sound trade-off between exploitation and exploration. In the proposed design, this is accomplished by modifying the number of genes that are mutated between generations, instead of considering a constant value of gene mutation as usual in GAs. The number of genes mutated has a direct impact on the exploration rate of the algorithm. The total number of offspring that can be generated from the g-th parent through the mutation process is given by (9), where m is the number of genes to mutate from the $g-th$ parent. Equation (9) is similar to (6) but instead of considering the total number of modules that must be allocated, it considers a subset of available modules that can be relocated in the mutated genes. Equation (9) also considers how m genes can be selected without repetition among the total number of N_K genes. The amount of ways in which the $g-th$ parent can be mutated to create a new offspring is given by:

$$N_p^g\left(m, N_g^{mut}\right) = \binom{N_K}{m} \cdot \binom{N_g^{mut} + m - 1}{m - 1} \tag{9}$$

The graph concerning equation (9) is shown in Fig. 5. It shows the curve has a concave shape, thus allowing the definition of the maximum offspring generation locus for each parent via mutations (black line in the figure). This locus of maximum offspring plays a key role in the definition of the mutation operator, as it defines the extent to which the exploration is performed within the search space during the creation of new generations from any given parent.

As shown in (9) the increase of the total number of offspring generated from the $g-th$ parent, considering one additional bus to mutate, is given by:

$$\begin{aligned} \Delta N_p^g &= N_p^g\left(m+1, N_g^{mut}\right) - N_p^g\left(m, N_g^{mut}\right) \\ \Leftrightarrow \Delta N_p^g &= N_p^g\left(m, N_g^{mut}\right) \cdot \frac{(m-m_1)(m-m_2)}{m \cdot (m+1)} \end{aligned} \tag{10}$$

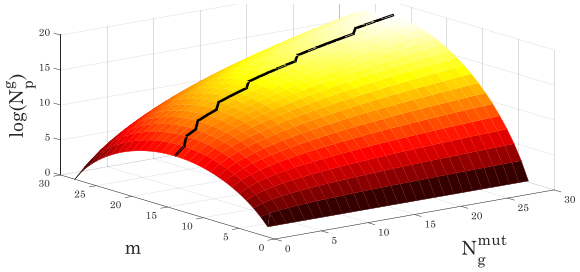

Fig. 5. *Number of possible offspring generated by a mutation operator.*

The roots m_1 and m_2 are given by the following expression:

$$m_{1,2} = \frac{N_K - N_g^{mut} - 1 \pm \sqrt{\left(N_K - N_g^{mut} - 1\right)^2 + 8N_K N_g^{mut}}}{4} \quad (11)$$

Since all numbers are strictly positive, it is clear that:

$$\sqrt{\left(N_K - N_g^{mut} - 1\right)^2 + 8N_K N_g^{mut}} \geq N_K - N_g^{mut} - 1 \quad (12)$$

So m_1 is always positive and m_2 is always negative. Thus, m_1 is the root determining the incremental trend of (10), that allows its maximum value in relation to m to be found, according to:

$$m\left(N_K, N_g^{mut}\right) = \left\lceil \frac{N_K - N_g^{mut} - 1 + \sqrt{\left(N_K - N_g^{mut} - 1\right)^2 + 8N_K N_g^{mut}}}{4} \right\rceil \quad (13)$$

where $\lceil \cdot \rceil$ represents the ceiling function. In other words, (13) determines the locus of maximum exploration for any given parent (black path in Fig. 5). Note that the result in (13) is only a function of the number of busbars where BESS modules can be allocated and the total number of modules that can be relocated to selected genes that will mutate. This makes the proposed GA general enough to be applied in any power system. The locus of maximum exploration allows counteracting variations in the exploitation throughout the mutations, as illustrated in Fig. 6. The figure shows an example of two busbars in which a total amount of α modules must be allocated. As such, the feasible search space is marked in red and each candidate is denoted as $Q_{i,j}$, where i defines the number of modules allocated in bus 1 and j the modules allocated in bus 2. One can simply extend the example to a bigger number of nodes.

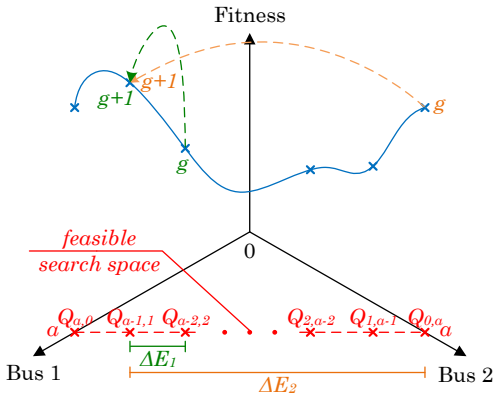

Fig. 6. *Mutation operator to counteract exploration.*

Exploitation can be measured as the difference in module allocations between two consecutive parents, in this case denoted by ΔE. One possible way of doing this is by comparing the allocated modules in each gene between the two candidates (i.e. $\Delta E_1 = 2$ and $\Delta E_2 = 2\alpha - 2$). This allows us to know the maximum and minimum values that exploitation can reach (in the example 0 and 2α) and it provides a fast method to measure it. By knowing ΔE, it is possible to adjust the exploration using (13) to define the amount m of genes to mutate in order to create the next generation of candidates. This in turn translates into an increase of the exploration when the exploitation rises; thus, avoiding a convergence to a local optimum. On the contrary, when the exploitation decreases, i.e. two consecutive parents are very different candidates from an allocation perspective, the exploration must decrease in order to improve the convergence time.

Finally, by means of (13) it is possible to adjust the exploration rate in each generation automatically, according to the following rule: *The search should aim to relocate those modules that were situated at the exact same distance between two consecutive parents*. Regarding the previous example, it explains that by computing $2\alpha - \Delta E$ in (13), it is possible to define the number of genes to mutate while maximizing the sets of candidates where the search can be performed.

The strategy presented offers the ideal trade-off between exploitation and exploration by incorporating a key characteristic from the power system (i.e. the short circuit levels) into the optimization problem.

6.3. Final remarks about the design of the GA

The design presented allows the GA to adapt to any power system by considering its inherent technical/dynamic characteristics, without needing to adjust the parameters during the evolution process (which determines the convergence rate and the quality of the solutions). In fact, the only parameter that the user needs to establish is the number of BESS modules that must be allocated. The number of BESS modules can be determined by planning studies performed ex-ante or from budget restrictions.

7. Case Study

The proposed methodology to allocate BESS modules for improving system stability was implemented in the 39-bus New England system [23]. The 39-bus New England system consists of 39 nodes and 10 conventional SGs. In this case study, we replaced three SGs by variable-speed wind turbine generators (WTG). A simplified diagram of the test network is shown in Fig. 7. The generator labelled as "G01" represents the interconnection of the system to the rest of the USA and Canada. Fig. 8 shows the short circuit level of the high voltage busbars of the system. Strong buses with a short circuit power greater than 5500 MVA are colored in green, while weaker ones (with short circuit levels below 4500 MVA) are marked in red.

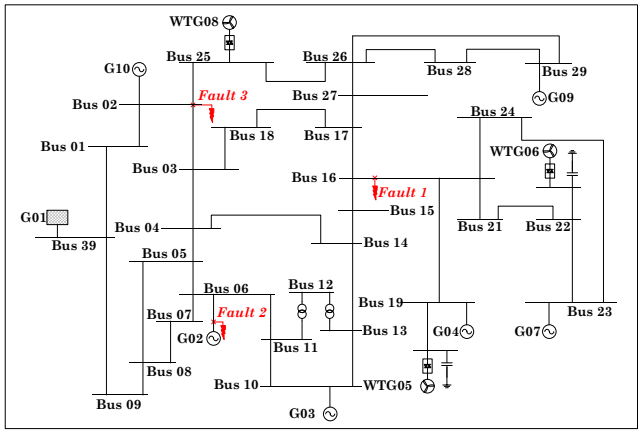

Fig. 7. *Network of the study case.*

The operation point considered for the BESS allocation task is characterized by 2386 MW of wind power, covering 39% of system demand (6097 MW). This operation point represents a worst-case scenario from a stability

perspective, i.e., a high penetration level of CBGT. The allocation task is performed considering three critical contingencies which lead to system instability (marked in red in Fig. 7). All contingencies represent critical cases from a stability perspective and their occurrences are considered to be equally probable. Hence, the same weighing factor is used in the optimization, i.e. $\lambda = 1$.

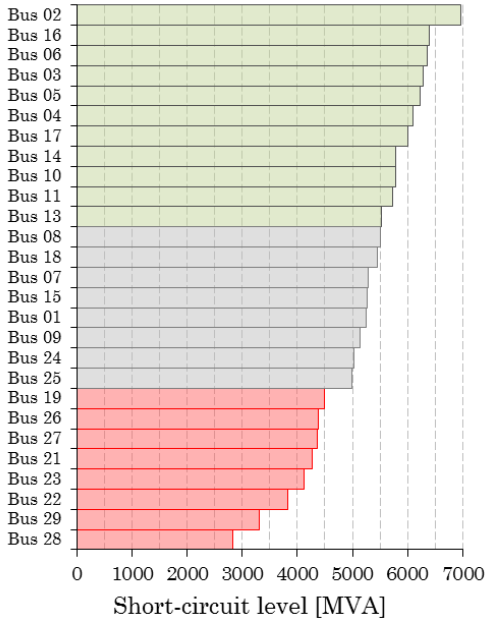

Fig. 8. *Short circuit levels of the network.*

8. Results

In this section we present the results obtained in the validation of the proposed GA and also those from a larger case study. The GA was implemented in the DIgSILENT PowerFactory software. The calculations were performed on a computer with two Intel(R) Xeon (R) E5–2630 v3 processors (2.4 GHz) and 32 GB of RAM.

8.1. Validation of the proposed GA

The objective of this validation is to verify that the proposed GA reaches similar solutions for different realizations of the algorithm. Since convergence to the optimum when using GA cannot be mathematically guaranteed, a statistical validation is proposed based on the behavior of the fitness function. With this aim, each of the following case studies was solved using a total of 100 independent simulations (runs). Each run was randomly initiated.

The first case study (base case) consisted of allocating 10 BESS modules in 10 possible busbars. The total BESS capacity installed was assumed to be 700 MW. In each run, 3000 candidates distributed in 100 generations (of 30 chromosomes each) were evaluated. Fig. 9 summarizes the results obtained for the fitness function in each generation. The solid line shows the average fitness of the best candidates found in each generation when all the runs had concluded. The dashed line at the top shows the maximum fitness value achieved in 100 runs while the bottom one represents the minimum value.

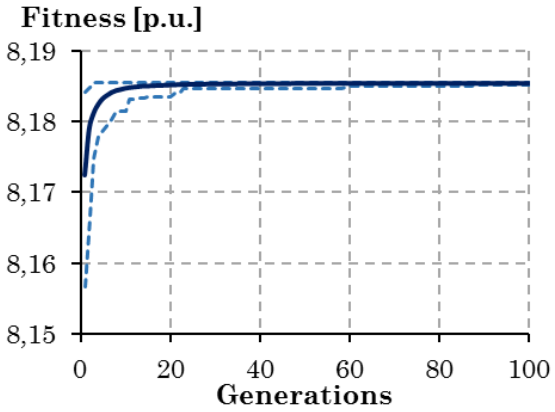

Fig. 9. *Maximum, minimum, and average value of the fitness function of the best candidate in each generation.*

The results of the base case showed that 97% of the runs reached the same final solution. The difference between the fitness values of the best and worst runs in the final generation was 0,004%. The 100 runs, equivalent to 300000 candidate evaluations, took 26972 seconds (7.5 hours) to be completed. The evaluation of each candidate took on average 89.91 milliseconds. These results show that the proposed algorithm systematically converges to solutions with similar properties from a stability point of view.

In order to evaluate the scalability of the proposed algorithm regarding the number of BESS modules to be allocated, four additional case studies (sensitivities) were considered. In the first sensitivity the number of BESS modules allocated was 20, which systematically increased by 10 in the following ones. Therefore, the last sensitivity consisted of allocating a total of 50 BESS modules. The number of possible busbars for allocating the modules, as well as the total BESS capacity to install (700 MW) remained fixed. An indicator of the scalability of the GA, regarding the number of BESS modules allocated, the ratio between the number of candidate solutions (size of the search space) and the standard deviation of the solutions provided by the GA in the last generation were used. The amount of candidate solutions for each case study can be determined using equation (8). This indicator allows one to evaluate how close the solutions provided by the GA are and how much they spread as the number of candidates increases, thus providing a measurement of how scalable the proposed algorithm is regarding the number of BESS modules that should be allocated.

Given these conditions, a total of 100 runs of the GA for each sensitivity were performed. Fig. 10 presents the value of the standard deviation of the solutions obtained with the GA as a function of the number of candidates. This figure shows that the standard deviation of the solutions provided by the GA increases along with an increasing number of allocation candidates. However, such increase follows a logarithmic rule. Although the search space experiences a combinatorial growth with each allocation scenario (according to equation (8)), the standard deviation of the fitness function grows logarithmically. This indicates that the number of modules can be increased to a certain extend without compromising the quality of the solution.

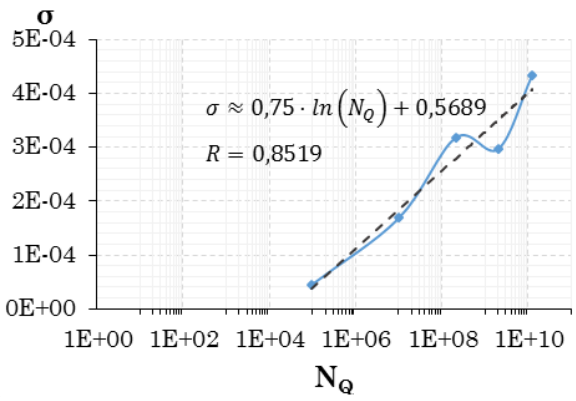

Fig. 10. *Convergence speed for the proposed GA.*

It is worth pointing out that the only parameters that needed to be adjusted were the number of generations and the amount of offspring per generation. In the base case study these parameters were determined based on several simulations of the algorithm. The influence of the parameters in the performance of the program as well as further sensitivity analysis (for example number of candidates versus degree of freedom) is beyond the scope of this paper. Nevertheless, the test simulations performed with a different number of busbars, as the degree of freedom allowed, showed that the time required to complete each candidate evaluation was almost the same (90 milliseconds). The main difference between the case studies is the number of generations required to reach convergence. Although it is not possible to define a general convergence criterion, the number of candidate evaluations can be set according to the simulation time available in order to reach good allocation schemes.

8.2. BESS allocation considering a higher number of candidate busbars

In this section, the BESS allocation problem considers 28 candidate busbars for the allocation of 20 BESS modules of 45 MW each, in the 39 bus New England System, is presented. The total BESS capacity is therefore 900 MW, which represents around one third of the total CBGT capacity. This 900 MW is equivalent to 13% of the total installed generation capacity without considering G01. This value was chosen based on the results obtained in [19], where cost-effective BESS capacities were found to be a 23% of the generation capacity for 50% of the renewable penetration. This result was obtained considering a stochastic multistage co-optimized BESS-transmission expansion plan.

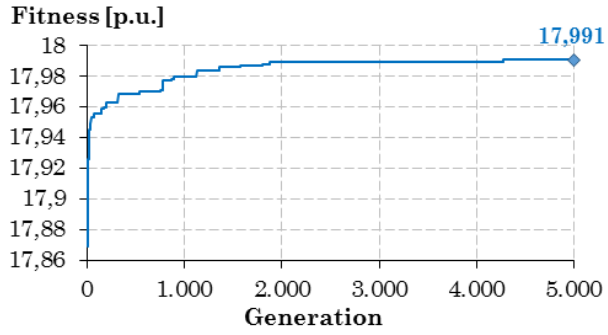

Fig. 11. *Fitness evolution over the optimization.*

Fig. 11 shows the evolution of the fitness function over 5000 generations of 30 candidates each. The computing time required to reach 5000 generations was 14236 seconds (4 hours). The evaluation of each candidate took on average 94 milliseconds, which is similar to the evaluation time obtained in the validation stage (90 milliseconds). As seen in Fig. 11, the fitness function values of the best candidate from each generation presents large variations during the first 2000 generations, and afterwards it tends towards a constant value. The final solution was reached after 4277 generations.

Fig.12 presents the allocation results including the number of BESS modules allocated at each candidate busbar. The busbars with high short circuit levels are highlighted in green and those with lower short circuit levels in red (see Fig. 8 for reference). From this figure it becomes clear that the GA not only allocates BESS modules in weak areas of the network but also in busbars with high short-circuit levels. This is the case with busbars 4 and 13, where one and five BESS modules are located respectively. This is –in principle– counterintuitive, since it is expected that the network reinforcement takes place mainly in weak areas, i.e. in those busbars with low short-circuit levels. On the one hand, this result can be explained by the fact that reinforcing strongly connected (highly meshed) busbars can have a positive effect over a wide network area, thus significantly improving the dynamic performance of the system as a whole. On the other hand, the allocation of BESS modules in strong busbars is also associated to its proximity to critical faults. This is the case, for instance, with fault 2. This fault is a short circuit at the terminals of generator G02 that makes this generator lose synchronism after 212.1 ms in the case without BESS. As seen in Fig. 12, when the optimization is executed considering this fault, the GA allocates one BESS module in busbar 4 despite that it is a strong busbar. Since this BESS module is not directly connected to bus 6 (where fault 2 occurs), it can considerably improve the voltage dips in the neighbouring busbars when this fault occurs (see Section 3, Fig. 2, b). Indeed, as will be shown in the next section, this BESS module in busbar 4 avoids the loss of synchronism of G02 during the occurrence of fault 2.

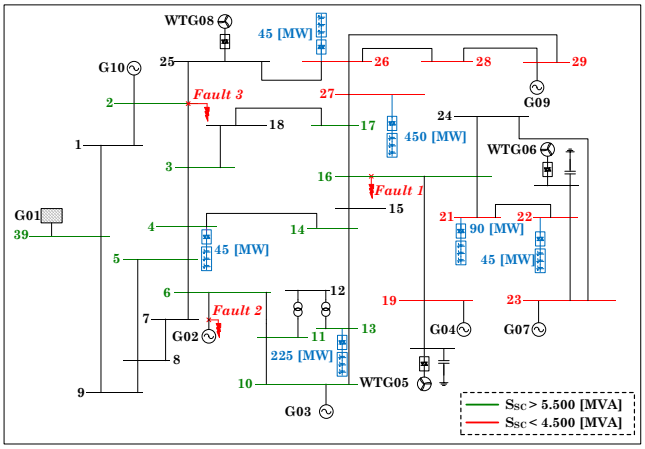

Fig. 12. *BESS allocation results using the proposed GA considering three faults.*

It is important to highlight that the decision to reinforce busbars with high short-circuit levels is strongly influenced by the distribution of the other BESS modules and by the location of the faults considered in the optimization.

To understand the relationship between the allocation results and the selected faults, the allocation task was performed in two additional cases: a) when only considering fault 1 and b) when only considering faults 1 and 3. As done before, in both cases 20 BESS modules were allocated by the GA. The results obtained in both cases are shown in Fig. 13.

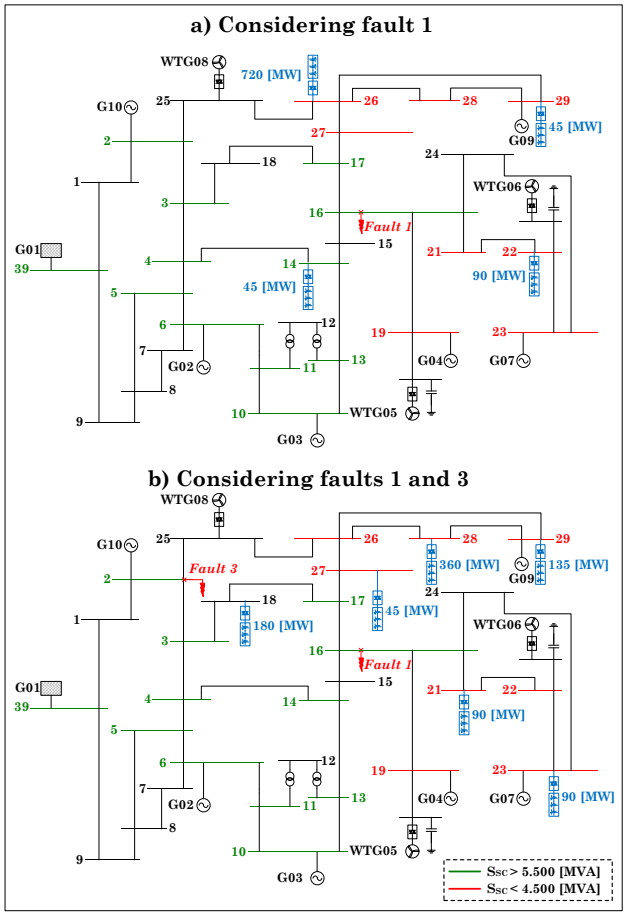

Fig. 13. *BESS allocation results using the proposed GA* ***a)*** *considering only fault 1;* ***b)*** *considering faults 1 and 3.*

Fig. 13 a) shows the BESS allocation obtained when only fault 1 is considered. Fault 1 is a short circuit at bus 16 (a strong bus) whose neighboring area is characterized by several buses with low short circuit levels (buses 19, 21, 22, 23, 26, 27, 28, and 29). Consequently, this short circuit has a wide system-effect, leading to a poor dynamic performance in the nearby area during and after the fault. Indeed, as will be shown in the next section, without BESS, this short circuit causes voltage instability after 160.6 ms which, in turn, leads to the loss of synchronism of G09. Because of this, when the GA considers only fault 1 (Fig. 13 a)), several BESS modules are allocated in weak busbars close to bus 16.

In the second case, when fault 1 and 3 are considered, the obtained BESS allocation is the one shown in Fig. 13 b). Fault 3 is a short circuit at bus 2 which causes significant voltage dips in busbars 26, 28 and 29, all of them with low short circuit levels. Busbars 28 and 29 are indeed extremely weak buses that form an isolated ring; connected to the rest of the system only through busbar 26. Accordingly, this area exhibits a poor dynamic performance after the fault clearance which, in turn, leads to the loss of synchronism of generator G09 (connected to busbar 29) in the case without BESS. To prevent this, the GA allocates some BESS modules in weak busbars near fault 3.

As expected, the comparison of figures 12 and 13 shows a dependency between the BESS allocation results and the faults considered in the optimization. Although the solutions shown are different from a module distribution perspective, they have two major similarities:

- Some of the BESS modules are always placed in the weakest busbars of the network. Concretely, in buses 21, 22, 26, and 27 when considering the three faults (Fig. 13), and in buses 22, 26, and 29 when considering only fault 1 (Fig. 13, a), and in buses 21, 23, 27, 28, and 29 when considering faults 1 and 3 (Fig. 13, b).
- Some BESS modules are allocated in busbars near the critical contingencies which leads to system instability regardless of the robustness level of the pertinent busbars.

8.3. Dynamic validation of the proposed GA

In this section we validate the solution obtained with the GA from a stability perspective. To do this, we performed time domain simulations to see the dynamic performance of the system during each fault considered in the optimization. The simulations are performed in DIgSILENT using a full dynamic model of the system. We consider three scenarios, all with a 39% of CBGT penetration:

- Scenario 1: baseline scenario without BESS.
- Scenario 2: scenario including 900 MVA of BESS (20 modules of 45 MVA each) distributed in the busbars of the system with renewable generation (busbars 34, 35, and 37). This would be one of the usual BESS allocation solutions adopted in planning exercises and economic operation assessments.
- Scenario 3: scenario including 900 MVA of BESS (20 modules of 45 MVA each) distributed in the load busbars of the system (in total 19 busbars). This would be another usual BESS allocation solution typically used in planning studies and economic operation assessments.
- Scenario 4: scenario including 900 MVA of BESS (20 modules of 45 MVA each), located in the network by means of the proposed GA.

Fig. 14 shows the angle evolution of critical machines for each considered contingency. Fig. 14 shows that the BESS allocation obtained by means of the proposed GA ensures system stability during all contingencies considered in the optimization. On the other hand, when the BESS are distributed either in the load busbars or at renewable generation points, stability cannot be sustained during fault 2 and 3. Only during fault 1 stability is ensured regardless of the BESS allocation that was used. This demonstrates that, from a stability perspective, BESS allocation decisions taken only considering economic criteria may have an equally poor dynamic performance as in the case without BESS. Moreover, distributing the BESS modules in load busbars or in buses with renewable generation, does not necessarily lead to an improvement in the system's stability and might even drive the system towards an unstable dynamic behaviour.

The performance of the BESS allocation was also verified in case of contingencies that were not included in the optimization. To do this, other faults (different from those considered in the optimization) were simulated. This allows the evaluation of the robustness of the obtained solution in

case other contingencies occur, which is of key importance due to the uncertain nature of the faults in power systems.

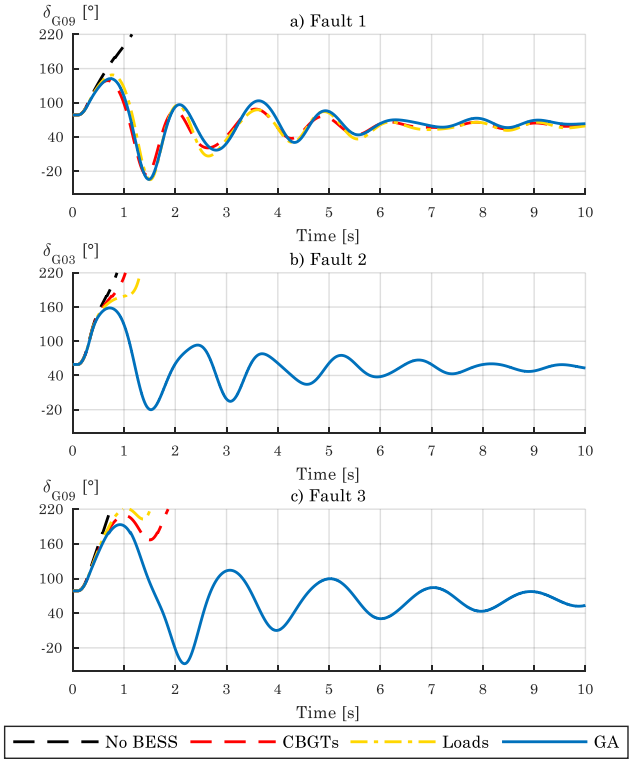

Fig. 14. a) *Angle of G09 during fault,* ***b)*** *Angle of G03 during fault 2,* ***c)*** *Angle of G09 during fault 3.*

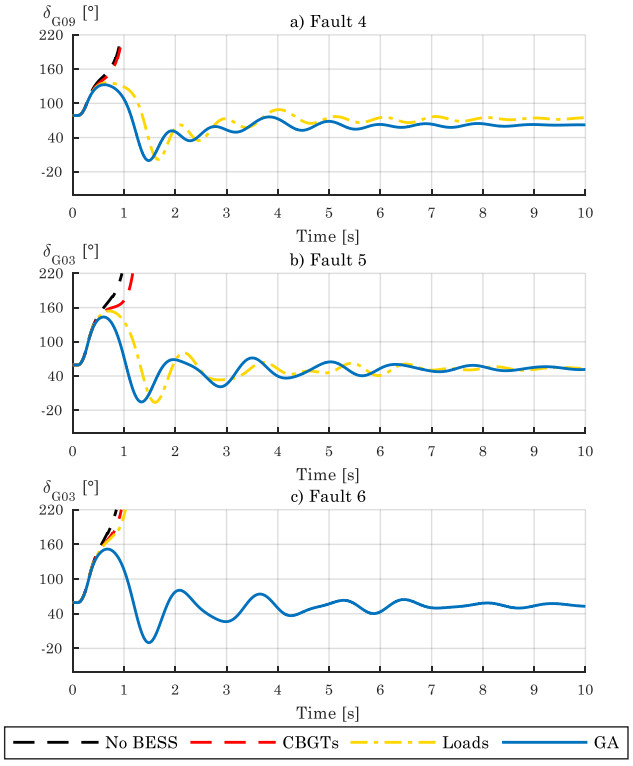

Fig. 15. a) *Angle of G09 during fault 4,* ***b)*** *Angle of G03 during fault 5,* ***c)*** *Angle of G03 during fault 6.*

Fig. 15 shows the results obtained in the following fault cases:

- Fault 4: a three-phase short-circuit at Bus 26
- Fault 5: a three-phase short-circuit at Bus 10
- Fault 6: a three-phase short-circuit at Bus 11

As shown in Fig. 15, the BESS allocation with the proposed GA leads to an outstanding dynamic performance of the system, even during faults that were not considered in the optimization. The fact that the system is stable in all cases highlights the robustness of the obtained solution. This is due to the worst case approach adopted in the optimization. On the other hand, when the BESS are co-located with renewable generation, the system is unstable in four of the six faults studied. The allocation of BESS modules in the load busbars is not much better: the system is unstable in three of the six faults. Similar results were found for other contingencies, which are ommited here in favor of brevity.

9. Conclusions

This paper proposes a novel methodology to allocate battery energy storage systems (BESS) in power systems in order to improve system stability. The proposed methodology exploits the fact that a reactive current injection by BESS modules during contingencies allows the improvement of short-term voltage and transient stability. The problem was addressed by means of a genetic algorithm (GA) specifically designed for the allocation problem. The optimization model uses transient voltages during selected fault events to quantify the stability improvement achieved by a particular BESS allocation. Although the transient voltages were calculated using traditional short circuit calculations (i.e. based on a steady state model of the system), the results obtained show that the improvements in this indicator are directly reflected in the enhancements achieved in power system dynamic performance and therefore also in system stability.

The BESS allocations that were obtained with the proposed GA, were capable of ensuring the system's stability during the contingencies that were considered in the optimization. Moreover, the obtained allocations led to an outstanding system dynamic performance even during faults that were not considered in the optimization. On the other hand, the dynamic simulations showed that co-locating the BESS units with renewable power plants or in load busbars does not necessarily allow it to maintain system stability during contingencies.

The results obtained have shown that an efficient BESS allocation decision for improving system stability must consider both, the weakest busbars of the network and areas prone to face stability problems even if these areas are strongly connected (highly meshed). Despite the promissory results obtained in this research, the selection of the critical contingencies and the effects of stability support capability in the life-cycle of the BESS, are still pending issues that require further research efforts.

10. Acknowledgments

The authors acknowledge the support of the Chilean Council of Scientific and Technological Research, CONICYT/FONDECYT/11160228, Fondap/ 15110019, and the Complex Engineering Systems Institute, ISCI (ICM-FIC: P05-004-F, CONICYT: FB0816), in this work.

References

[1] IEEE/CIGRE joint task force on stability terms and definitions: 'Definition and classification of power system stability', *IEEE Trans. Power Syst. vol. 19, no. 3,* pp. 1387-1401, 2004.

[2] Bill Parks, U.S. Department of Energy: 'Transforming the Grid to Revolutionize Electric Power in North America'," *Edison Electric Institute's Fall 2003 Transmission, Distribution and Metering Conference,* 2003.

[3] A. Gavrilovic: 'AC/DC system strength as indicated by short circuit ratios', *International Conference on AC and DC Power Transmission,* London, UK, 1991, pp. 27-32.

[4] AEMO: 'Fact Sheet: System Strength', available at: https://www.aemo.com.au/-/media/Files/Electricity/NEM/Security_and_Reliability/Reports/2016/AEMO-Fact-Sheet-System-Strength-Final-20.pdf

[5] NERC: 'Short-Circuit Modeling and System Strength', *White Paper,* February 2018.

[6] NERC: 'Integrating Inverter Based Resources into Weak Power Systems Reliability Guideline', June 2017.

[7] S. Huang, J. Schmall, J. Conto *et al*: 'Voltage control challenges on weak grids with high penetration of wind generation: ERCOT experience', *2012 IEEE Power and Energy Society General Meeting,* San Diego, 2012, pp. 1-7.

[8] R. A. Walling, E. Gursoy and B. English: 'Current contributions from Type 3 and Type 4 wind turbine generators during faults', *2011 IEEE Power and Energy Society General Meeting,* Detroit, MI, USA, 2011, pp. 1-6.

[9] N. Tleis: 'Power systems modelling and fault analysis, 1st ed.', Oxford, Eng.: Newnes Power Engineering, 2008.

[10] EEE/NERC Task Force on Short-Circuit and System Performance Impact of Inverter Based Generation: 'Impact of Inverter Based Generation on Bulk Power System Dynamics and Short-Circuit Performance', *IEEE Power & Energy Society,* July 2018.

[11] R. Go, F. Munoz and J. Watson: 'Assessing the economic value of co-optimized grid-scale energy storage investments in supporting high renewable portfolio standards', *Applied Energy 183,* p. 902–913, 2016.

[12] S. Wogrin and D. Gayme: 'Optimizing Storage Siting, Sizing, and Technology Portfolios in Transmission-Constrained Networks', *IEEE Trans. Power Syst., vol. 30, no. 6,* pp. 3304-3313, 2015.

[13] A. Kanchanaharuthai, V. Chankong and K. Loparo: 'Transient stability and voltage regulation in multimachine power systems vis- à -vis STATCOM and battery energy storage', *IEEE Trans. Power Syst., vol. 30, no. 5,* p. 2404–2416, 2015.

[14] S. Baros, M. D. Ilić: 'Multi-Objective Lyapunov-based control of a STATCOM/BESS', *Innovative Smart Grid Technologies Conference, Washington DC,* 2015.

[15] S. Chen, H. Gooi and M. Wang: 'Sizing of Energy Storage for Microgrids', *IEEE Transactions on Smart Grid, vol. 3, no. 1,* pp. 142-151, 2012.

[16] I. Konstantelos and G. Strbac: 'Valuation of Flexible Transmission Investment Options Under Uncertainty', *IEEE Trans. Power Syst., vol. 30, no. 2,* pp. 1047-1055, 2015.

[17] F. Zhang, Z. Hu and Y. Song: 'Mixed-integer linear model for transmission expansion planning with line losses and energy storage systems', *IET Generation, Transmission & Distribution, vol. 7, no. 8,* pp. 919-928, 2013.

[18] S. Dehghan and N. Amjady: 'Robust Transmission and Energy Storage Expansion Planning in Wind Farm-Integrated Power Systems Considering Transmission Switching', *IEEE Transactions on Sustainable Energy, vol. 7, no. 2,* pp. 765-774, 2016.

[19] T. Qiu, B. Xu, Y. Wang *et al.*: 'Stochastic Multistage Coplanning of Transmission Expansion and Energy Storage', *IEEE Trans. Power Syst., vol. 32, no. 1,* pp. 643-651, 2017.

[20] T. Das, V. Krishnan and J. McCalley: 'Assessing the benefits and economics of bulk energy storage technologies in the power grid', *Applied Energy 139,* p. 104–118, 2015.

[21] V. Virasjoki, P. Rocha, A. Siddiqui *et al.*: 'Market Impacts of Energy Storage in a Transmission-Constrained Power System', *IEEE Trans. Power Syst., vol. 31, no. 5,* pp. 4108-4117, 2016.

[22] N. Li and K. Hedman: 'Economic Assessment of Energy Storage in Systems With High Levels of Renewable Resources', *IEEE Transactions on Sustainable Energy, vol. 6, no. 3,* pp. 1103-1111, 2015.

[23] S. Chakrabarti and E. Kyriakides: 'Optimal Placement of Phasor Measurement Units for Power System Observability', *IEEE Trans. Power Syst., vol. 23, no. 3,* pp. 1433-1440, 2008.

[24] J. Machowski, J. Bialek and J. Bumby: 'Power System Dynamics: Stability and Control', 2nd Edition. John Wiley & Sons, 2008.

[25] P.M. Anderson: 'Power System Protection', McGraw Hill, 1999.

[26] K. Kawabe and A. Yokoyama: 'Effective Utilization of Large-Capacity Battery Systems for Transient Stability Improvement in Multi-Machine Power System', *PowerTech, 2011 IEEE Trondheim,* 2011.

[27] K. Kawabe and A. Yokoyama: 'Improvement of Angle and Voltage Stability by Control of Batteries Using Wide-Area Measurement System in Power Systems', *Innovative Smart Grid Technologies (ISGT Europe), 2012 3rd IEEE PES International Conference and Exhibition on,* 2012.

[28] I. Erlich, F. Shewarega, S. Engelhardt *et al.*: 'Effect of wind turbine output current during faults on grid voltage and the transient stability of wind parks', *2009 IEEE PES General Meeting,* 2009.

[29] J. Machowski, S. Robak, P. Kacejko *et al.*: 'Short-circuit power as important reliability factor for power system planning', *Power Systems Computation Conference (PSCC), Wroclaw, Poland,* 2014.

[30] M. Eremia and M. Shahidehpour: 'Handbook of Electrical Power System Dynamics: Modeling, Stability, and Control', Wiley-IEEE Press, 2013.

[31] I. Erlich, U. Bachmann: 'Grid code requirements concerning connection and operation of wind turbines in Germany', *Power Engineering Society General Meeting, 2005. IEEE,* June 12-16, 2005 Page(s):2230 – 2234

[32] C. Rahmann, D. Ortiz-Villalba, R. Álvarez and M. Salles: 'Methodology for selecting operating points and contingencies for frequency stability studies', *2017 IEEE Power & Energy Society General Meeting,* Chicago, IL, 2017, pp. 1-5.

[33] L. G. W. Roberts, A. R. Champneys, K. R. W. Bell *et al:* 'Analytical Approximations of Critical Clearing Time for Parametric Analysis of Power System Transient Stability', *IEEE Journal on Emerging and Selected Topics in Circuits and Systems,* vol. 5, no. 3, pp. 465-476, Sept. 2015.

[34] T. L. Vu, S. M. Al Araifi, M. S. El Moursi *et al*: 'Toward Simulation-Free Estimation of Critical Clearing Time', *IEEE Transactions on Power Systems,* vol. 31, no. 6, pp. 4722-4731, Nov. 2016.

[35] Michael Pertl, Tilman Weckesser, Michel Rezkalla *et al*: 'A decision support tool for transient stability preventive control', *Electric Power Systems Research,* vol 147, 2017, pp. 88-96

[36] D. E. Goldberg: 'Computer implementation of a genetic algorithm', in *Genetic Algorithms in Search, Optimization & Machine Learning,* Addison-Wesley Publishing, 1989.

[37] D. Reid: ‘Genetic algorithms in constrained optimization’, *Mathematical and Computer Modelling, vol. 23, no. 5,* pp. 87-111, 1996.
[38] W. Macready and D. Wolpert: ‘Bandit problems and the exploration/exploitation tradeoff’, *IEEE Transactions on Evolutionary Computation, vol. 2, no. 1,* pp. 2-22, 1998.
[39] J. Grefenstette: ‘Optimization of Control Parameters for Genetic Algorithms’, *IEEE Transactions on Systems, Man, and Cybernetics, vol. 16, no. 1,* pp. 122-128, 1986.